Journal of Asian Earth Sciences 40 (2011) 1121–1130

Contents lists available at ScienceDirect

Journal of Asian Earth Sciences

journal homepage: www.elsevier.com/locate/jseaes

The $\delta^{18}O$ and $\delta^{13}C$ records in an aragonite stalagmite from Furong Cave, Chongqing, China: A-2000-year record of monsoonal climate

Hong-Chun Li [a,b,c,*], Zhong-Hong Lee [a], Nai-Jung Wan [a], Chuan-Chou Shen [c], Ting-Yong Li [d], Dao-Xian Yuan [d], Yong-Heng Chen [b]

[a] Department of Earth Sciences, National Cheng-Kung University, Tainan 70101, Taiwan, ROC
[b] School of Environmental Science & Engineering, Guangzhou University, Guangzhou 510006, China
[c] High-Precision Mass Spectrometry and Environment Change Laboratory (HISPEC), Department of Geosciences, National Taiwan University, Taipei 10617, Taiwan, ROC
[d] School of Geographical Sciences, Southwest University of China, Chongqing 400715, China

ARTICLE INFO

Article history:
Available online 30 June 2010

Keywords:
Aragonite stalagmite
Oxygen and carbon isotopes
Furong Cave
Chongqing
Paleoclimate

ABSTRACT

A 7-cm long aragonite stalagmite, FR0510-1, from Furong Cave, Chongqing, was dated by ^{210}Pb and ^{230}Th methods, revealing a-2000-year record of climate history under the influence of the East Asian Monsoon. The FR0510-1 record resembles Dongge Cave DA record on 10–100-year scales, but quite different from the Wanxiang Cave WX42B record, indicating that while stalagmite $\delta^{18}O$ record represents local/regional moisture change, spatial variability of the monsoonal rainfall over eastern China must take into account. During the past 2000 years, climate in Chongqing was relatively wet in the intervals of 50 BC–AD 250, AD 1150–1450 and AD 1600–1950, and relatively dry during the periods of AD 250–1150 and AD 1450–1600. Dry conditions were prevailing over the Medieval Warm Period, whereas wet climates were dominant during the most time of the Little Ice Age in Chongqing area.

1. Introduction

Owning to its high-resolution multi-proxy records and absolute chronological control with high-precision ^{230}Th dating, stalagmite record has been received extensive attention during the past 20 years, in the field of Holocene–Pleistocene paleoclimate and paleoenvironment (e.g., McDermott, 2004; Fairchild et al., 2006; Henderson, 2006). For example, stalagmite $\delta^{18}O$ records were used to reconstruct changes in East Asian summer monsoon (EASM) during the Holocene (Li et al., 1998; Ku and Li, 1998; Paulsen et al., 2003; Wang et al., 2005; Hu et al., 2008a,b; Zhang et al., 2008; Cosford et al., 2008, 2009) and during the late Pleistocene (Wang et al., 2001, 2008; Yuan et al., 2004; Dykoski et al., 2005; Li et al., 2005). Studies about other monsoonal systems have also been done by using stalagmite records, e.g., on Indian monsoon (ISM) history (Denniston et al., 2000; Burns et al., 2003; Fleitmann et al., 2003, 2007; Berkelhammer et al., 2010) on the north African monsoon (Bar-Matthews et al., 2000) and on the north American monsoon (Polyak and Asmerom, 2001; Lachniet et al., 2004). By comparing stalagmite $\delta^{18}O$ records to changes in solar radiation, high latitude temperature recorded in polar ice cores, sea surface temperature (SST) and oceanic volume (or sea level) recorded in marine sediments, it has been found that regional climates reconstructed are closely linked to global changes.

That the Hulu Cave $\delta^{18}O$ record from Nanjing resembled the solar insolation curve and calibrated the older part of the Greenland ice core chronology (Wang et al., 2001), indicates an orbital forcing and a teleconnection between East Asian Monsoon and Northern Hemisphere climate change. When solar insolation increases in the Northern Hemisphere, rising temperature leads to enhanced East Asian summer monsoon (EASM) strength, which brings more rainfall and/or more maritime air mass over the eastern China. As a consequence of enhanced summer monsoon, a light speleothem $\delta^{18}O$ will be resulted (Wang et al., 2001, 2005, 2008; Yuan et al., 2004; Zhang et al., 2008). However, in the vast eastern China, modern spatial rainfall variability clearly exists. It is very common that dryness/wetness in North China and the Yangtze River drainage basin occurred oppositely in the past 60 years (Zhang et al., 2010). Unlike the Indian Monsoon which has an apparently positive correlation with the Indian rainfall, EASM plays a complicated role on the precipitation over eastern China. There is no simple correlation between the EASM strength and rainfall intensity based on recent multi-decadal observations (Zhang et al., 2010). On annual-to-centennial time scales, the following questions for East Asian Monsoon evolution in the late Holocene are still unanswered: Is

* Corresponding author at: Department of Geosciences, National Taiwan University, Taipei 106, Taiwan, ROC. Tel.: +886 2 33662929; fax: +886 2 23636095.
E-mail address: hcli1960@ntu.edu.tw (H.-C. Li).

1367-9120/$ - see front matter © 2010 Elsevier Ltd. All rights reserved.
doi:10.1016/j.jseaes.2010.06.011

it sound that strong EASM would bring high precipitation over the eastern China? Are warm/wet and cold/dry the only monsoonal climatic modes? Does stalagmite $\delta^{18}O$ record reflect changes in regional monsoonal intensity or in local moisture source?

Most published stalagmite records are calcite stalagmite. The use of aragonite stalagmite for paleoclimate study is still controversial (Fairchild et al., 2006). This is because aragonite may be not stable enough under certain temperature and pressure conditions, so that phase-change or re-crystallization may occur after its formation (Frisia et al., 2002). In such a circumstance, isotopic fractionation may obscure climatic signals in the stalagmites. Isotopic fractionation factors of aragonite–water and calcite–water are different. If a stalagmite contains different portion of calcite and aragonite at different depths, it is difficult to interpret the variations in isotopic values as changes in paleoclimate and paleoenvironment (Frisia et al., 2002; Lachniet, 2009). In this study, we present $\delta^{18}O$ and $\delta^{13}C$ records of an aragonite stalagmite collected from Furong Cave in southeast Chongqing, China. We use ^{210}Pb and ^{230}Th dating methods to build up the chronology of the stalagmite. High-resolution $\delta^{18}O$ record of the stalagmite will compare with local instrumental and historic records for understanding natural dynamics of the stable isotopic compositions of the aragonite stalagmite and regional climatic condition. The study area is located in the upper reaches of the Yangtze River basin, and its climate is strongly influenced by the East Asian monsoon. The study results will help us to answer the fore-mentioned questions.

2. Background information of the study area and sample

2.1. Climate of the area

Located in Wulong County in the southeast Chongqing, Furong Cave (29°13′44″N, 107°54′13″E) lies on the east bank of Furongjiang River which is a secondary branch of the Yangtze River (Fig. 1). The direct distance of Furong Cave to Chongqing City is about 130 km, so that its climate is basically similar to that of Chongqing. As the largest city of China with a population of more than 30 million people, Chongqing has annual precipitation of 1086 mm/year (AD 1891–1993) and annual mean temperature of 18.3 °C (AD 1905–1993) (Fig. 2). Although the rainy season in Chongqing area begins in April, rainfalls in spring months (March-to-May) are mainly contributed by local storms which account for ~26% of the annual precipitation (Fig. 3). Under the EASM influence, moisture from Pacific contributes the summer rainfall with a peak reached in June. Rainfall during the summer months (June-to-August) takes ~41% of the annual precipitation. With the influence of ISM, the rainfall in the autumn months of the area reaches the second peak in September, accounting for ~27% of the annual precipitation (Fig. 3). Hence, although the EASM plays an important role on the precipitation of the study area, other components such as ISM and local feedback obscure the direct correlation between the EASM strength and precipitation amount. For instance, a positive correlation can be found between West North Pacific Monsoon (WNPM) index and summer rainfall of Chongqing

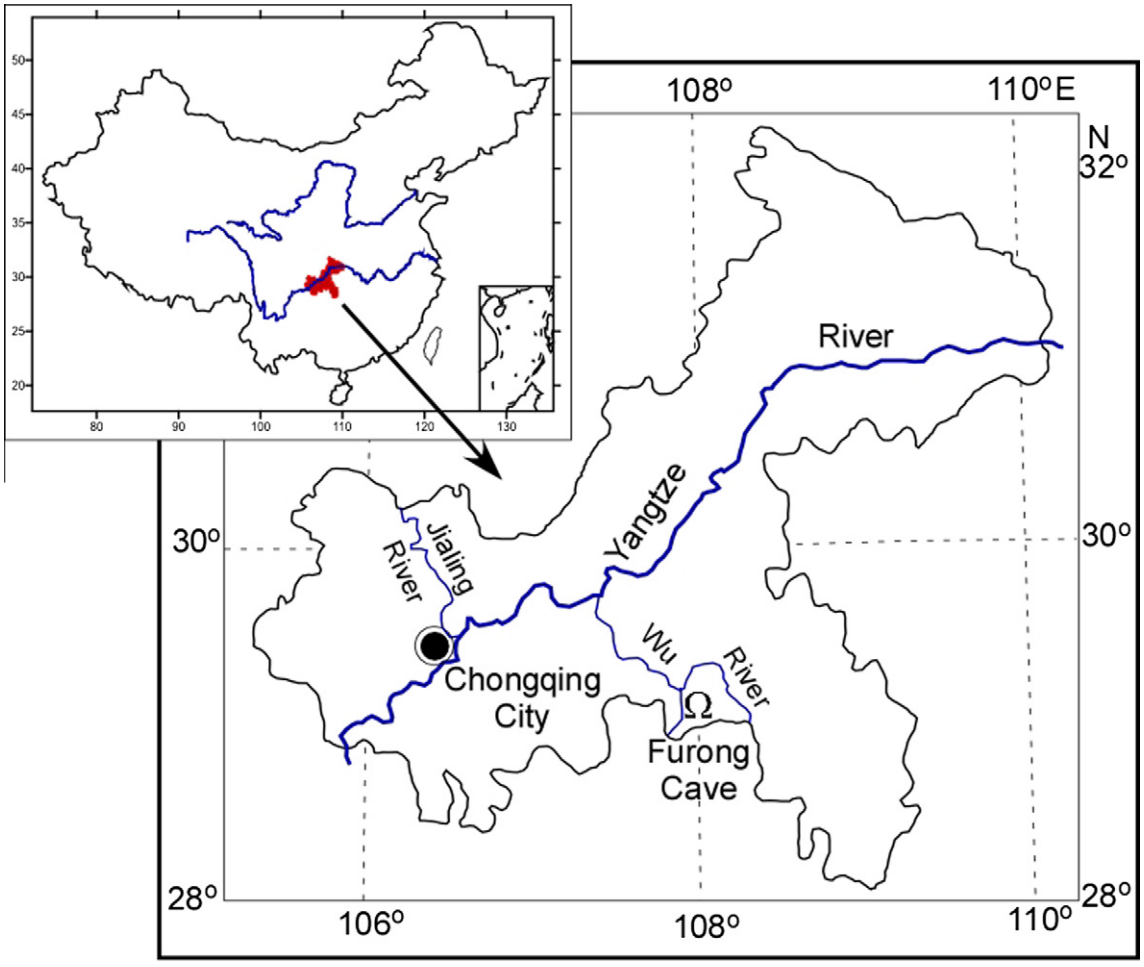

Fig. 1. Locations of the study area and Furong Cave. Chongqing is in the mid-upper reach of the Yangtze River with the secondary tributary rivers of Jialingjiang River and Wujiang River. Climate there is hot and humid during the summer under the influence of the summer monsoons. Furong Cave is about 130 km southeast of Chongqing City.

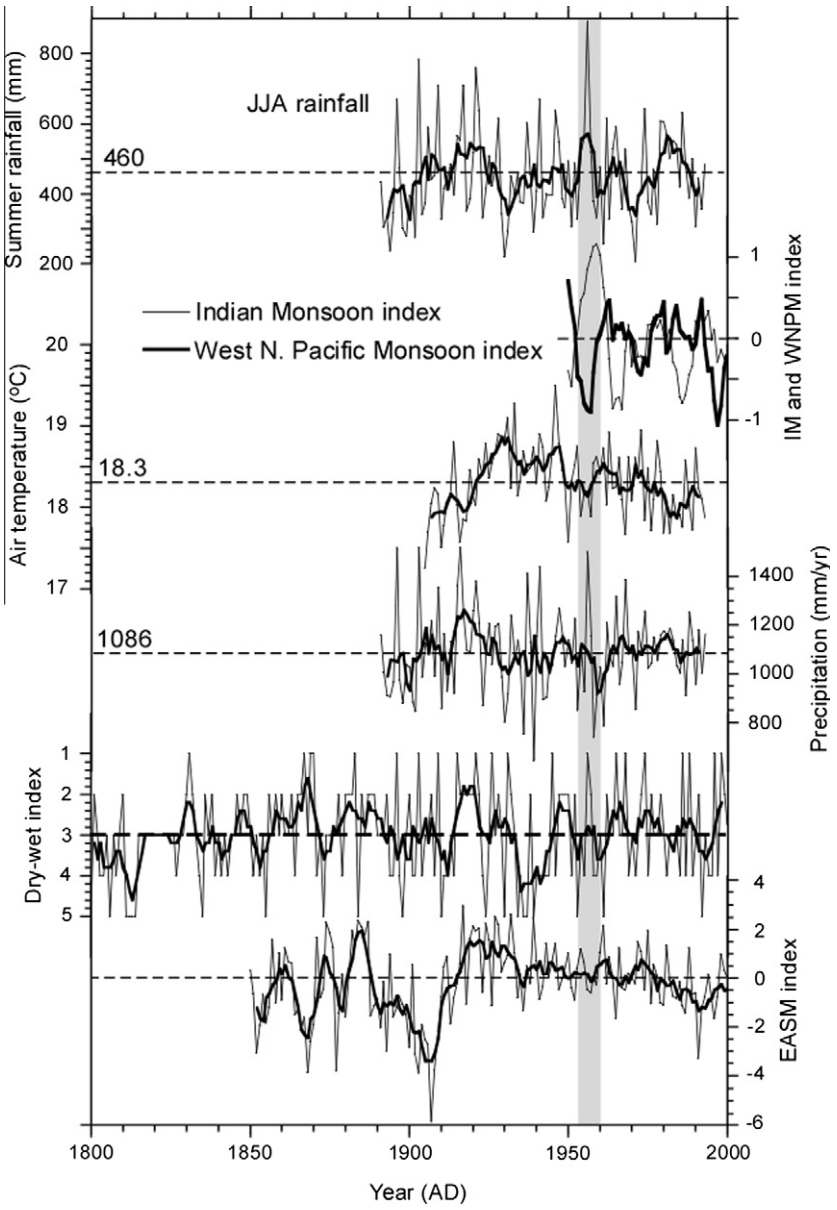

Fig. 2. Comparisons among the instrumental record, historic record of Chongqing and monsoon indexes. The broken lines denote the average values of the records: (a) summer rainfall (June–August) in Chongqing, (b) Indian (thin line) and West North Pacific (thick line) summer (JJA) monsoon index (Redraw from Wang (2006)), (c) annual mean air temperature of Chongqing, (d) annual precipitation of Chongqing (*Note*: Data (a), (c) and (d) source from: China Meteorological Data Sharing Service System), (e) historic dryness/wetness index of Chongqing (Chinese Academy of Meteorological Sciences, 1981; Zhang et al., 2003), and (f) East Asian summer monsoon index (IPCC, 2007).

during AD 1960–1990, but negatively correlated during AD 1950–1960 (Fig. 2). Instead, a strong positive correlation existed between ISM index and the summer rainfall during AD 1950–1960. Given that the WNPM and ISM operate independently, it is difficult to see a direct correlation between Chongqing rainfall and either WNPN or ISM. In winter time, cold and dry weather appears in the area under the influence of the winter monsoon (Fig. 3).

The monthly air temperature ranges from 7.6 °C in January to 28.5 °C in August (Fig. 3), showing warm/wet and cold/dry patterns. However, on 1–10-year scales, temperature and rainfall are generally negatively correlated (Fig. 2). Unlike the global warming trend, the long-term temperature trend of Chongqing is declined since AD 1925. Although the local climate belongs to subtropical warm and wet monsoonal climates, one may not obtain a direct correlation between rainfall and monsoonal intensity, and response of rainfall to temperature on 1–10-year scales.

Few studies on paleoclimate during Holocene and late Pleistocene in Chongqing area have been reported. Speleothem records are the major paleoclimate recorders in the area (He et al., 2007; Li, 2007; Li et al., 2006, 2007, 2008a,b). A low-resolution stalagmite $\delta^{18}O$ record from Xinya Cave in the northeast Chongqing is the only published Holocene record in Chongqing (Li et al., 2006). Therefore, the Holocene paleoclimate history especially during the past 2000 years in the study area remains unclear.

2.2. Furong Cave

Wulong County contains a typical karst gorge area, where a famous karst system including natural karst bridges (Tianshengqiao), dolines (Tiankeng), karst gorges and caves was assigned as a World Natural Heritage site by the United Nations Special Coordinator Office (UNSCO) in 2007. The bedrocks are mainly Cambrian limestone

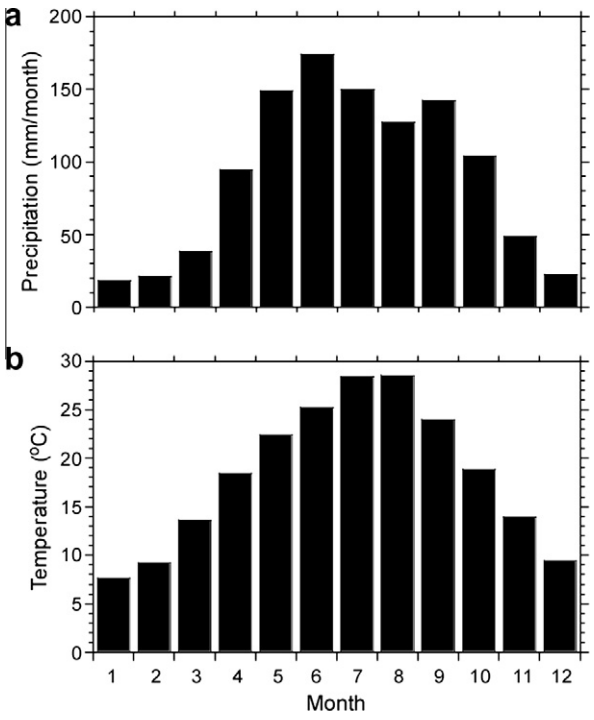

Fig. 3. Monthly mean precipitation (AD 1891–1993) and air temperature (AD 1905–1993) of Chongqing. Rainfall peaks appeared in June and September are brought by the East Asian summer monsoon from Pacific and the Indian summer monsoon from Indian Ocean, respectively.

and dolomite. The area is covered with extensive vegetation, and has large topographical reliefs from the mountaintop down to the river, a maximum of 1000 m.

The entrance of Furong Cave is 260 m above the Furongjiang River, with an elevation of 480 m above sea level (a.s.l.). The relatively thick epikarst above Furong Cave ranges from 300 m to 500 m, whereas the covered soil is relatively thin, ranging 0–20 cm. The cave is currently 2.8 km long in which about 1.8 km opens to public since AD 1994. With abundant fresh speleothem deposits and dripping waters, the cave is enclosed with 90–100% humidity which provides good conditions for oxygen isotopic fractionation between water and carbonate. Throughout a main tunnel of the cave, four large chambers with 30–50 m in height are presence. The cave temperature recorded by an automatic data-logger over 1 year has been constantly 16.0–16.3 °C after a long-term hydrological monitor program started in AD 2005.

2.3. Stalagmite FR0510-1

Stalagmite FR0510-1 was collected in the deep part of the cave at the #2 monitoring station in October of 2005. The sample is 7.3-cm in length, with pure and clear carbonate deposition (Fig. 4a). No lamination band can be observed under microscope, and no growth hiatus can be found either. Active dripping water exists on the stalagmite surface when collected, indicating the stalagmite was in growth position. The sample has been analyzed for XRD, ^{210}Pb dating, ^{230}Th dating, and IRMS carbon and oxygen isotopic measurement (Fig. 4a).

3. Analytical methods

The ^{210}Po alpha method was used for the ^{210}Pb dating (Baskaran and Iliffe, 1993; Li et al., 1996). In order to obtain an excess ^{210}Pb profile, we sampled the top layer of the stalagmite with caution, by scraping off and collecting powders from the surface, beneath the surface and at 4 mm depth (samples FR0510-1-A to -C in Table 1). About 0.2 g powder of each sample drilled from the stalagmite were dissolved by concentrated HNO_3, and spiked with ^{209}Po. Organics in the solution was oxidized with H_2O_2. The clear solution was added ascorbic powder to remove the influence of Fe. The Po was self-precipitated onto silver plate in 0.1 N HCl solution under 80 °C water bath for 4–6 h. The silver plate was counted for ^{210}Po and ^{209}Po by ORTEC alpha spectrometer. The counting uncertainty varies with the activities of each isotope, but the error depends mainly on the counts of ^{210}Po. The ^{210}Pb dating results are listed in Table 1.

The ^{230}Th dating was performed at the High-precision Mass Spectrometry and Environment Change Laboratory (HISPEC) of the National Taiwan University. All chemical procedures are followed the method described in Shen et al. (2002, 2003). The

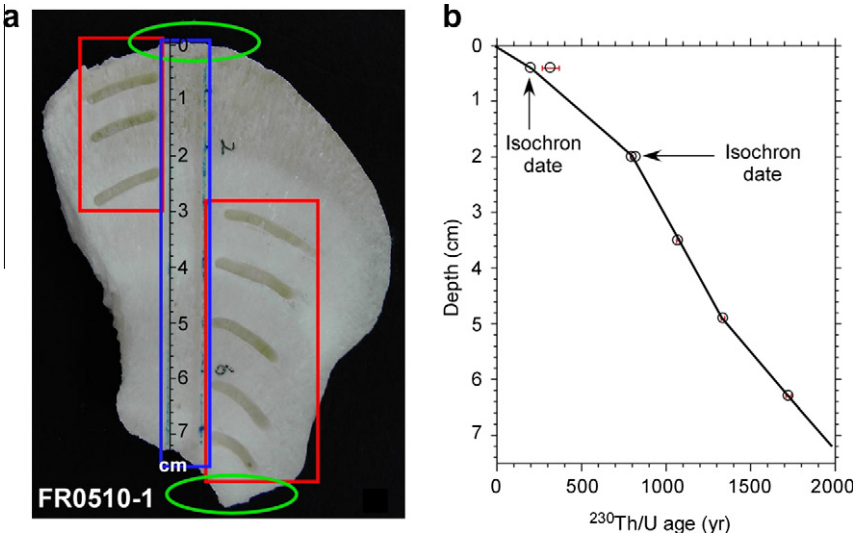

Fig. 4. (a) Photo of stalagmite FR0510-1. Subsamples have been analyzed for XRD (sampling position shown by green circles), ^{210}Pb dating (in the red boxes), ^{230}Th dating (yellow layers), and IRMS carbon and oxygen isotopic measurement (blue column) and (b) age-depth relationship of FR0510-1 reconstructed by ^{230}Th ICPMS dating. The isochron age at the top shows significant difference from the single date, indicating initial ^{230}Th/^{230}Th is much higher than 4.4 ppm in this sample.

Table 1
^{210}Pb dating results of stalagmite FR0510-1 from Furong Cave.[a]

Sample	Distance from top (mm)	Range (mm)	Measured ^{210}Pb (dpm/g)	Error (dpm/g)	Excess ^{210}Pb (dpm/g)
FR0510-1-A[a]	0.1	0.01	59.4	3.0	58.0
FR0510-1-B[a]	0.5	0.1	32.2	1.9	31.8
FR0510-1-Pb-001	1	0.5	28. 4	1.1	28.0
FR0510-1-C[a]	4	0.1	12.03	0.87	11.62
FR0510-1-Pb-002	11	1	0.55	0.13	0.15
FR0510-1-Pb-003	20	1	0.49	0.11	
FR0510-1-Pb-004	30	1	0.71	0.12	
FR0510-1-Pb-005	40	1	0.170	0.055	
FR0510-1-Pb-006	48	1	0.78	0.15	
FR0510-1-Pb-007	60	1	0.048	0.038	
FR0510-1-Pb-008	70	1	0.197	0.068	
FR0510-1-Pb-009	73	1	0.285	0.075	

[a] Denote that the samples were from the second sampling time.

instrument for Th and U isotopic analyses is Finnigan Neptune multi-collector inductively coupled plasma mass spectrometer (MC-ICP-MS) (Frohlich et al., 2009). The analytical precision of the samples is very high mainly due to high U contents and low Th detritus. We have also conducted isochron dating techniques for two layers. Calculations of U–Th isotopic data and ^{230}Th and isochron dates were described in Shen et al. (2008). All ^{230}Th dating results are listed in Table 2.

The X-ray Diffraction analyses on stalagmite FR0510-1 were carried out in the Department of Earth Sciences at National Cheng-kung University (NCKU). The results show that stalagmite FR0510-1 is pure aragonite without detectable calcite.

Stable isotope samples were drilled along the growth axis of stalagmite FR0510-1 at 0.25 mm interval. A total of 299 samples were analyzed for δ^{18}O and δ^{13}C using a Kiel III automated carbonate device connected on a Finnigan Delta XP Plus gas isotopic ratio mass spectrometer (IRMS) in the Laboratory of Stable Isotope Geochemistry, NCKU, Taiwan. The reference CO_2 gas has been calibrated with international standards of NBS19, NBS18 and LSVEC. A working standard, NCKU1 made from a pure stalagmite, has been run with every 5–7 samples to monitor the instrument. The long-term precisions (1σ) are 0.06‰ for δ^{13}C and 0.08‰ for δ^{18}O based on 532 runs of NBS19. Stable isotope data are reported relative to the V-PDB standard at 25 °C.

4. Results and discussion

4.1. ^{210}Pb dating

^{210}Pb activity is very low below 4 mm depth of the stalagmite (Table 1, Fig. 5), indicating the stalagmite grew very slow. Only the top samples at depths 0.1–4 mm of stalagmite FR0510-1 exhibits excess ^{210}Pb. Figure 5 shows the total ^{210}Pb profile and exponential decay of excess ^{210}Pb. Based on the fitting of excess ^{210}Pb decay trend, an average growth rate of 0.0583 mm/year is calculated for the upper 10 mm in the stalagmite. However, as no data between 4 and 10 mm depths, the calculated growth rate relies on the data point at 10-mm depth. If the supported ^{210}Pb was reached at a depth between 4 and 10 mm, then the growth rate of 0.0583 mm/year would be overestimated. In fact, the growth rate built up by the ^{230}Th ages is ~0.041 mm/year (below), indicating the growth rate given by the ^{210}Pb dating is overestimated. Therefore, we do not use this growth rate for chronological calculation. Nevertheless, the ^{210}Pb dating results enable us to learn that: (1) carbonate deposit above the 4 mm depth should be younger than 100 years and (2) the growth rate of FR0510-1 is relatively low compared to general growth rates of 0.1–1 mm/year of stalagmites in south China (Liu et al., 2005; Tan et al., 2002).

4.2. ^{230}Th dating

Table 2 shows U–Th isotopic data and ^{230}Th dates, including two isochron data at depths of 4 mm and 20 mm. In general, the U contents of the samples are relatively high, ranging 280–1400 ppb. Expect the samples from the top layer, all samples contain low Th, indicating minimum influence of initial ^{230}Th. For these samples with low Th levels of 4–20 ppt, the corrected ages are the same as the uncorrected ones. Four isochron subsamples from 4 mm depth have relatively high ^{232}Th contents of 8000–12,000 ppt. In Fig. 6, we plot U and Th isotopic activity ratios to obtain radiogenic ratios. The slope and intercept of ^{230}Th/^{232}Th–^{238}U/^{232}Th plot (Fig. 6a and c) serve as radiogenic ^{230}Th/^{238}U and initial ^{230}Th/^{232}Th ratio, respectively. The initial ^{234}U/^{238}U ratios of the isochron samples are from the slopes of ^{234}U/^{232}Th–^{238}U/^{232}Th plot (Fig. 6b and d). With these "authigenic" (detrital free) ratios, we are able to calculate the "true" ages. For the isochron data set at 4 mm depth, corrected ^{230}Th/^{238}U is 0.0083 which yield an isochron age of 200 years. The initial ^{230}Th/^{232}Th ratio of the subsamples at 4 mm depth is 12.4 ppm

Table 2
ICPMS ^{230}Th/U results of stalagmite FR0510-1.[a]

Sample	Depth (mm)	^{238}U ppb	^{232}Th ppt	δ^{234}U[b] Meas.	$\left(\frac{^{230}Th}{^{238}U}\right)$	$\left(\frac{^{230}Th}{^{232}U}\right)$	Age[d] Uncorr.	Age[e] Corr.	$\delta^{234}U_o$[c] Corr.
1FI1-01	4	1398 ± 1	12537 ± 47	3379.0 ± 5.3	0.0140 ± 0.0003	4.79 ± 0.09	351 ± 6	200 ± 30	3400 ± 5
1FI1-02	4	1441 ± 2	9416 ± 35	3398.6 ± 6.4	0.0131 ± 0.0003	6.15 ± 0.12	327 ± 6		
1FI1-03	4	1375 ± 2	8356 ± 29	3448.6 ± 6.5	0.0131 ± 0.0002	6.59 ± 0.11	322 ± 5		
1FI1-04	4	966 ± 1	12,281 ± 46	3479.9 ± 6.9	0.0186 ± 0.0003	4.48 ± 0.10	455 ± 10		
1FI2-01	20	741 ± 1	80.9 ± 7.5	3812.1 ± 5.1	0.0348 ± 0.0002	973 ± 91	791 ± 6	800 ± 20	3820 ± 5
1FI2-02	20	757 ± 1	240.6 ± 7.2	3803.3 ± 5.5	0.0343 ± 0.0002	330 ± 10	783 ± 5		
1FI2-03	20	688 ± 1	221.0 ± 6.5	3803.3 ± 5.5	0.0349 ± 0.0002	332 ± 10	796 ± 5		
1FI2-04	20	636 ± 1	42.4 ± 6.4	3777.5 ± 6.5	0.0358 ± 0.0002	1641 ± 249	820 ± 5		
1FS-01	35	443 ± 0.1	4.3 ± 7.6	3627.8 ± 6.3	0.0453 ± 0.0004	13,880 ± 24,470	1072 ± 9	1072 ± 10	3639 ± 6
1FS-02	49	367 ± 1	20.0 ± 6.4	3555.6 ± 7.3	0.0556 ± 0.0004	3112 ± 996	1338 ± 10	1338 ± 10	3569 ± 7
1FS-03	63	276 ± 0.1	4.5 ± 7.8	3379.0 ± 5.3	0.0680 ± 0.0007	12,557 ± 21,752	1725 ± 17	1725 ± 20	3346 ± 7

[a] ^{230}Th/^{238}U and ^{230}Th/^{232}Th ratios are expressed activity ratio. Analytical errors are 2σ of the mean.

[b] $\delta^{234}U = ([^{234}U/^{238}U]_{activity} - 1) \times 1000$.

[c] $\delta^{234}U_{initial}$ corrected was calculated based on ^{230}Th age (T), i.e., $\delta^{234}U_{initial} = \delta^{234}U_{measured}\ X\ e^{\lambda 234 * T}$, and T is corrected age.

[d] $[^{230}Th/^{238}U]_{activity} = 1 - e^{-\lambda 230 T} + (\delta^{234}U_{measured}/1000)[\lambda_{230}/(\lambda_{230} - \lambda_{234})](1 - e^{-(\lambda 230 - \lambda 234)T})$, where T is the age.

[e] Age corrections were calculated using an ^{230}Th/^{232}Th atomic ratio of 4 (±4) ppm. Those are the values for a material at secular equilibrium, with the crustal ^{232}Th/^{238}U value of 3.8. The errors are arbitrarily assumed to be 100%. Decay constants are 9.1577×10^{-6} year^{-1} for ^{230}Th, 2.8263×10^{-6} year^{-1} for ^{234}U, and 1.55125×10^{-10} year^{-1} for ^{238}U (Cheng et al., 2000).

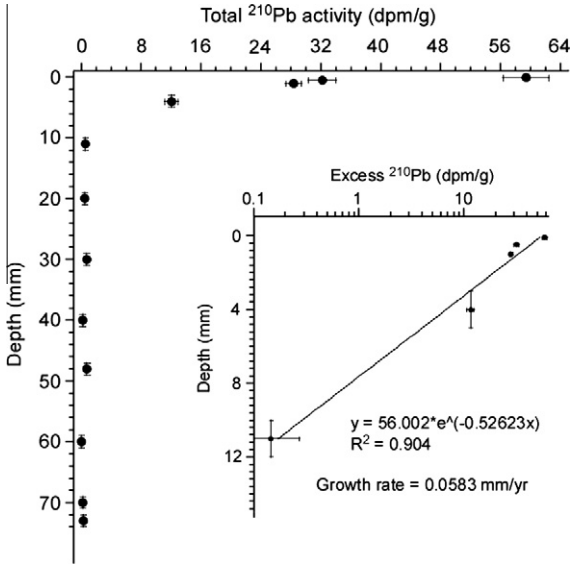

Fig. 5. Total ^{210}Pb profile (large figure) and excess ^{210}Pb profile (small figure) in FR0510-1. The excess ^{210}Pb activity is calculated by total ^{210}Pb activity minus the average total ^{210}Pb in the samples below 10 mm depth from where the ^{210}Pb becomes the supported ^{210}Pb.

calculated from an activity ratio of 2.29 which is the intercept of plot Fig. 6a. The isochron age of 200 ± 30 years at 4 mm depth does not agree the ^{210}Pb result which indicates the age of <100 years at 4 mm depth. Two reasons can be sued for the explanation of this disagreement: (1) powders from about 2–3 mm thick layer used for the ^{230}Th dating, so that the 4 mm depth is not accurate enough. The age of 200 ± 30 years is a mean age of 100–300 years. At any way, the isochron age is calculated by the computer program at HISPEC. We adopt this age for the chronology reconstruction. The other isochron age is 810 years for coeval subsamples at 20 mm depth given by the program calculation. However, the intercept of the isochron plot Fig. 6c is −16.7. In principle, $(^{230}Th/^{232}Th)_a$ ratio cannot be negative, and the corrected ^{230}Th age should be smaller than the uncorrected ^{230}Th age. The negative intercept is caused by the large uncertainty of the $(^{230}Th/^{232}Th)_a$ ratio of sample 1FI2-04, 1641 ± 249. If we reduce this ratio to 1580, then the intercept becomes 3.0 and the slope becomes 0.0346 which yields an age of 785 years. Therefore, we take a mean age of 800 ± 20 years between 783 (1FI2-01) and 820 years (1FI2-04) for the 20 mm depth. Based on these ^{230}Th dates, we establish the chronology throughout the entire stalagmite spanning the past 2050 years (Fig. 4b). The chronology of the stalagmite is established using linear interpolation between ^{230}Th dates. The average growth rate of stalagmite FR0510-1 is ~0.041 mm/year, smaller than 0.0583 mm/year that is obtained from the ^{210}Pb dating. The growth rate suggests that the ^{210}Pb-inferred rate of 0.0583 mm/year is overestimated due to lack of data points between 4 and 10 mm depths.

4.3. $\delta^{18}O$ record of FR0510-1

FR0510-1 δ^{18}O values range from −6.2 to −7.2‰. We evaluate oxygen isotopic fractionation by using measured cavewater δ^{18}O and cave temperature. Table 3 lists the average δ^{18}O and dissolved inorganic carbon (DIC) δ^{13}C values at several monitoring stations (Li, 2007). Using the pool water δ^{18}O of −7.06‰ at the monitoring site #2 where from Stalagmite FR0510-1 was collected, and cave temperature of 16.5 °C, we can calculate aragonite δ^{18}O under

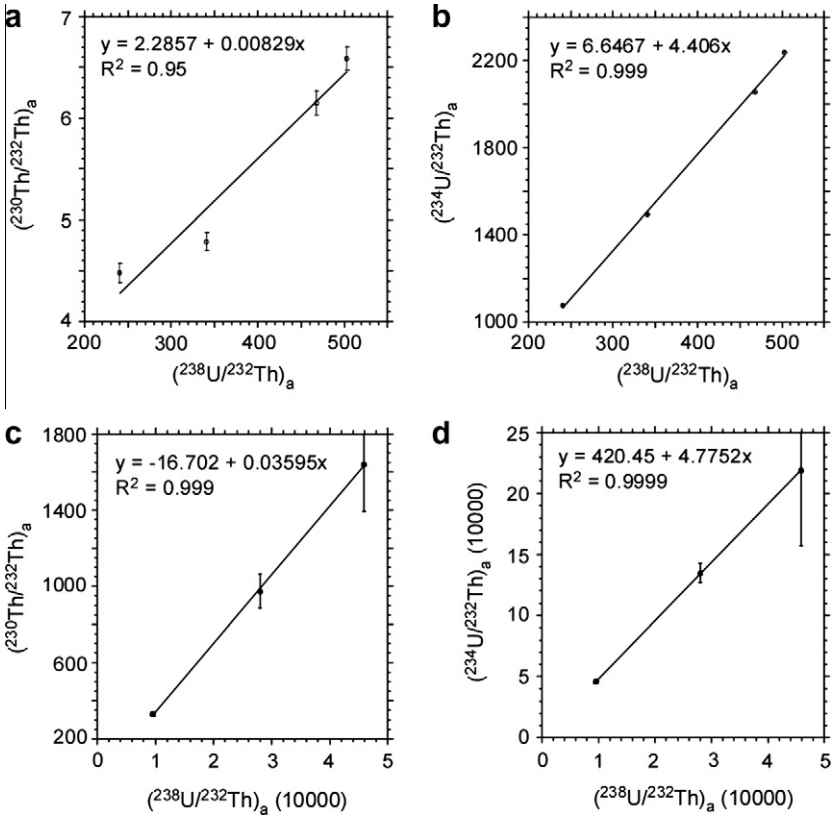

Fig. 6. U–Th isochron plots of subsamples at 4 mm and 20 mm depths from FR0510-1. The authigenic Th and U radioisotopic ratios of each sample are determined by these plots.

isotopic equilibrium fractionation by the equation of Patterson et al. (1993),

$$1000 \ln \alpha = \delta^{18}O_{aragonite} - \delta^{18}O_{water} = 18.56 \times 1000/T - 33.49 \quad (1)$$

where α is the $^{18}O/^{16}O$ fractionation factor between aragonite and water. T is depositional temperature in Kelvin (K). Both $\delta^{18}O_{aragonite}$ and $\delta^{18}O_{water}$ are in SMOW. The relationship between SMOW and PDB is:

$$\delta^{18}O_{PDB} = 1.03086 * \delta^{18}O_{SMOW} - 30.86 \quad (2)$$

The calculated aragonite $\delta^{18}O$ is −5.99‰ (PDB) under isotopic equilibrium fractionation, agreeing with the $\delta^{18}O$ of −6.28‰ in the top of FR0510-1 within uncertainty. Thus, we believe that the aragonite stalagmite grew in oxygen isotopic equilibrium.

Stalagmite $\delta^{18}O$ in monsoonal regions such as in eastern China has been treated as a proxy of rainfall amount variability (e.g., Li et al., 1998; Wang et al., 2001; Yuan et al., 2004) though changes in $\delta^{18}O$ of moisture source, shift of rainy season, and air temperature can affect stalagmite $\delta^{18}O$ (Li et al., 1998; McDermott, 2004; Fairchild et al., 2006). In order to confirm the $\delta^{18}O$ record of FR0510-1 as a paleo-precipitation proxy, we compare the historic dryness/wetness index (D/WI) of Chongqing with the FR0510-1 $\delta^{18}O$ record. The D/WI of Chongqing since AD 1799 was reconstructed from historic documents (Chinese Academy of Meteorological Sciences, 1981; Zhang et al., 2003), which was calibrated with the instrumental record of modern precipitation (AD 1891–1993) (Fig. 2). The D/WI reconstruction was mainly based on instrumental records of summer rainfall (May–September) and historic materials selected from Local Governmental Records, published historic literatures and royal written documents. Index 3 reflects normal condition which means no flooding or drought event with good harvest year. Index 2 is used for the case that heavy rainfall leads to local flooding in a single season. Index 1 represents intensive flooding occurred in a broad region with longer period causing serious damages and life losses. Indexes 4 and 5 are used for dryness situations similar to Indexes 2 and 1, respectively. For instrumental records in a station, Index 3 equals the average May–September rainfall (R) over the years of that instrumental record and its standard deviation (σ). When summer rainfall in a specific year is $>(R + 1.17\sigma)$, then the D/W index defines as 1. When the summer rainfall is between $(R + 0.33\sigma)$ and $(R + 1.17\sigma)$, the D/W index will be 2. Similarly, Indexes 5 and 4 are for conditions when the rainfalls are $<(R - 1.17\sigma)$, and between $(R - 0.33\sigma)$ and $(R - 1.17\sigma)$, respectively. Although the reconstruction of DWI before instrumental record may contain bias depending on the quality of historic documents, the accurate chronology and clear physical meaning make it valuable. The FR0510-1 $\delta^{18}O$ record of the last 200 years using ^{230}Th chronology was plotted in Fig. 7. Detailed comparison between the $\delta^{18}O$ record and D/WI record is difficult due to the decadally-resolved FR0510-1 $\delta^{18}O$ data and its age uncertainty. However, light $\delta^{18}O$ values are generally corresponding to wet climates, and vice versa. The comparison is better on the 11-year running average curve, and after AD 1870. As the ^{230}Th of 200 years is somehow older than the "true" age which has been discussed before, the older portion of the $\delta^{18}O$ record in Fig. 7 contains larger error.

In Fig. 8, $\delta^{18}O$ values of stalagmite FR0510-1 during the periods of 50 BC–AD 250, AD 1150–1450 and AD 1600–1950 are generally below (lighter than) the average of the 2000-year record, reflecting wet climates. During the intervals of AD 250–1150 and AD 1450–1600, the $\delta^{18}O$ values are normally heavier than the average, illustrating dry climates. The $\delta^{18}O$ record is also characterized with decadal-centennial fluctuations, showing detailed climatic dynamics, with lighter $\delta^{18}O$ swing in wet condition; and vice versa. The major feature of the FR0510-1 $\delta^{18}O$ record shows that dry climates were prevailing over the Medieval Warm Period (MWP), whereas wet climates were dominant during the most time of the Little Ice Age (LIA) in Chongqing area. Considering that more and more evidence shows that MWP and LIA were global events, warm and cold conditions in Chongqing might be corresponding to MWP and LIA, respectively. The warm/dry and cold/wet climatic patterns appeared in Chongqing during MWP and LIA illustrate that on 10–100-year scales such patterns are not rare in monsoonal regions.

The $\delta^{13}C$ of FR0510-1 has a range from −5‰ to 0.5‰ with most values heavier than −4‰ (Fig. 8). These heavy $\delta^{13}C$ values are way out of the $\delta^{13}C$ range (−12‰ to −6‰) in the C3 plants dominated area (McDermott, 2004). Since the influencing factors on the $\delta^{13}C$ are too complicated and the $\delta^{13}C$ record of FR0510-1 may not reflect surface vegetation change, we do not discuss the $\delta^{13}C$ record further in this paper.

4.4. Comparison of FR0510-1 $\delta^{18}O$ record with other stalagmite $\delta^{18}O$ records

Over the past 5 years, several high-resolution, Holocene $\delta^{18}O$ records with reliable chronology control in the eastern China have been generated, i.e., DA record from Dongge Cave in Guizhou

Table 3
Average $\delta^{18}O$ and DIC $\delta^{13}C$ values of the cavewaters in Furong Cave.[a]

Sample location	Type	Ave. $\delta^{13}C$ (‰, V-PDB)	Ave. $\delta^{18}O$ (‰, SMOW)	No. of months (no. of samples)
1# dripping water monitoring station	Drip water	−10.8 ± 1.1	−6.77 ± 0.14	21
Pool nearby 2# monitoring station	Pool water	−8.3 ± 2.2	−7.06 ± 0.25	21
3# dripping water monitoring station	Drip water	−11.17 ± 0.99	−7.02 ± 0.11	16
Pool nearby 4# monitoring station	Pool water	−7.7 ± 2.0	−7.36 ± 0.11	15
6# monitoring station, above the cave	Spring water	−10.1 ± 3.0	−7.05 ± 0.53	16

[a] Date summarized from Li (2007). The standard deviations are calculated from all measured samples from the monitoring months.

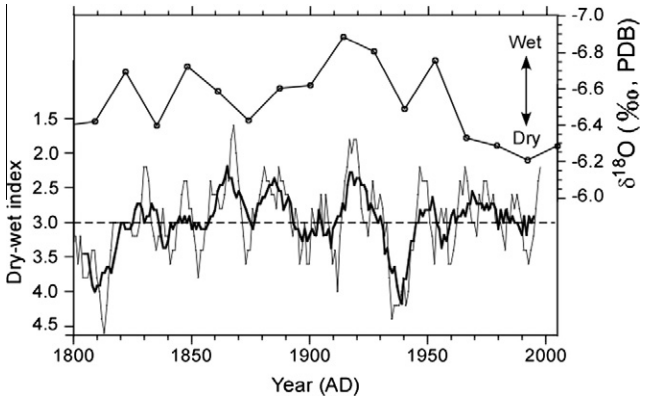

Fig. 7. Comparison of the ^{230}Th-dated FR0510-1 $\delta^{18}O$ record with the historic dryness/wetness index of Chongqing during AD 1800–2000. For the D/WI curve, the thin line is the 5-year running average and the thick line is 11-year running average.

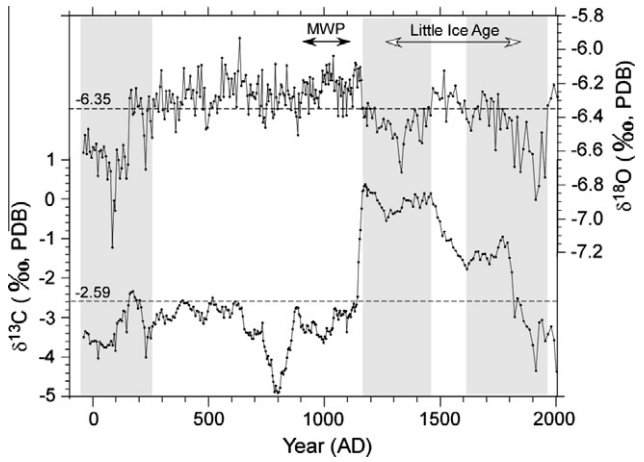

Fig. 8. The $\delta^{18}O$ and $\delta^{13}C$ records of FR0510-1 over the past 2000 years (see Section 4).

(Wang et al., 2005) Heshang Cave record in Hubei (Hu et al., 2008a,b) and WX42B record from Wanxiang Cave in Gansu (Zhang et al., 2008). The Dongge Cave record with the chronology <20 year uncertainty was compared with the radiocarbon curve which reflects the variability of solar irradiance (Wang et al., 2005). The Wanxiang Cave record with <10 year uncertainty was used to interpret changes in Chinese dynasty under climatic impact over the past 2000 years (Zhang et al., 2008). All these caves are located in the monsoonal region of the eastern China. The comparison between FR0510-1 $\delta^{18}O$ record with these records indicates that FR0510-1 $\delta^{18}O$ of Furong Cave record resembles DA $\delta^{18}O$ record of Dongge Cave on centennial scale, but certainly different from the other two (Fig. 9). There is no reason to attribute chronological uncertainties to the discrepancies among the curves on 10–100-year scales. The climatic conditions in terms of dryness/wetness must bear regional differences. In view of changes in precipitation trend over 1956–2000 of China, both Furong and Dongge Caves are located in the sites that the precipitation had increasing trend, whereas Wanxiang Cave had decreasing trend (Fig. 10). The features of the comparison on 10–100-year scales are: (1) spatial difference of rainfall variability as well as regional disparity of the relationship between rainfall and EASM intensity over eastern China does not allow existence of uniformed speleothem $\delta^{18}O$ records in different areas; and (2) there is no simple correlation between East Asia summer monsoon strength and rainfall intensity over the entire eastern China (Zhang et al., 2010).

It is interesting to see that the Furong Cave record and Wanxiang Cave record are somewhat anti-phasing during AD 500–1500 (Fig. 9). Recent study by Berkelhammer et al. (2010) showed that an Indian stalagmite record from Dandak Cave was strongly correlated with the Wanxiang Cave record (Fig. 9). If the Wanxiang Cave record was affected mainly with the Indian summer monsoon, whereas the Furong Cave and Dongge Cave records were influenced more by the EASM, the two monsoon systems may have opposite trends during some periods (Fig. 2) and/or different

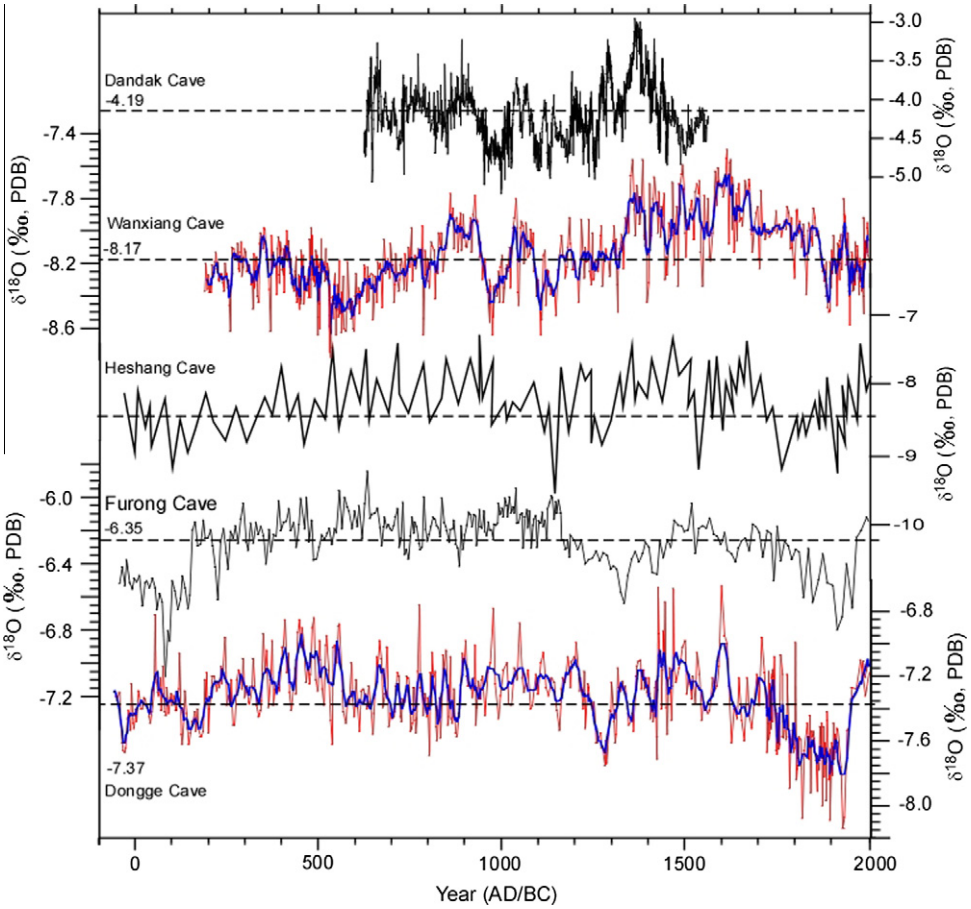

Fig. 9. Comparison of four well-dated stalagmite $\delta^{18}O$ record in the eastern China and one record from east central India over the past 2000 years, including Dongge Cave record (Wang et al., 2005), Wanxiang Cave record (Zhang et al., 2008), Heshang Cave record (Hu et al., 2008a,b), Dandak Cave (Berkelhammer et al., 2010) and Furong Cave record (this study).

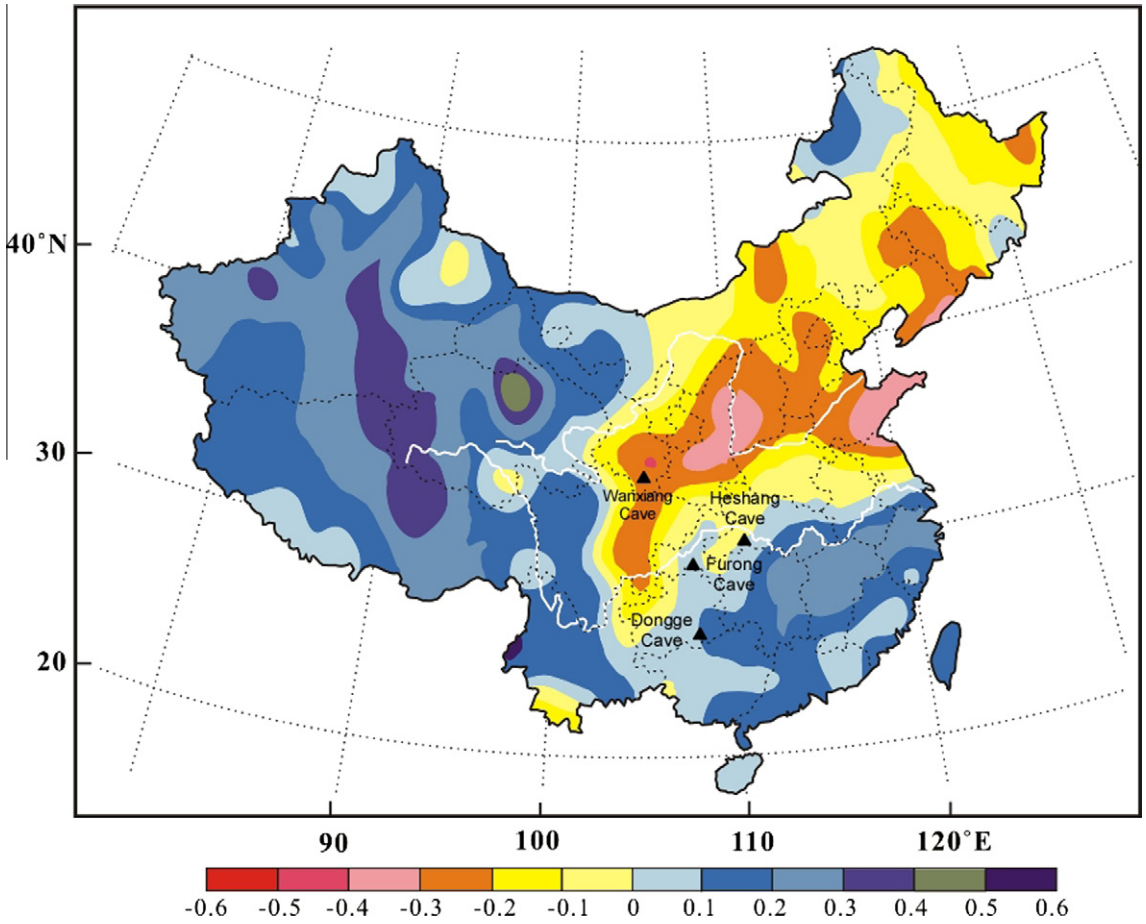

Fig. 10. Precipitation trend in China over 1956–2002. Color with positive values denotes precipitation increase. Tri-angles exhibit cave locations (redraw from Ding and Ren, 2008).

effects on the summer rainfall in north and south China. Berkelhammer et al. (2010) interpreted their record as evidence of SST variation in the North Atlantic, but not solar variability, to be the main driving force for persistent multidecadal variability of the ISM. In this regard, the debate on the relationships of solar variability-the EASM strength-summer rainfall on decadal to centennial scales in eastern China are far from settled.

5. Conclusions

Aragonite stalagmite FR0510-1 provides a-2000-year climatic history of Chongqing in mid-upper drainage area of Yangtze (Changjiang River). The record resembles the DA $\delta^{18}O$ record from Dongge Cave in southeastern Guizhou, indicating that two sites have similar precipitation trend under the influence of East Asia Monsoon. Over the past 2000 years, apparent discrepancies exist between the speleothem $\delta^{18}O$ records from south of Yangtze River (Furong and Dongge Cave records) and the $\delta^{18}O$ record from north of Yangtze River where Wanxiang Cave is located though precipitation in both regions is under strong influence of EASM. Dry climates occurred during the Medieval Warm Period, shown by heavier $\delta^{18}O$ values in the FR0510-1 record; and wet climatic conditions appeared dominantly during the Little Ice Age in Chongqing area. On 10–100-year scales, climatic patterns in the monsoonal regions of China also present warm/dry and cold/wet features. One should not interpret speleothem $\delta^{18}O$ records from a single location to represent changes in monsoon or rainfall intensity over a broad area of eastern China.

Acknowledgements

Funding for this study was provided by the Science Council of Taiwan (NSC 97-2628-M-006-014 and 98-2116-M-006 -003), the National Natural Science Foundation of China (Grant Nos. 40672202 and 40802035) and Special research grant for Academician from Chongqing Science and Technology Commission (Grant No. 20037835). Funding for ^{230}Th dating at the HISPEC was supported by the NSC Grants (98-2116-M-002-012 and 98-2611-M-0092-006 to CCS). We thank Prof. H.-R. Qing at University of Regina, Canada and another anonymous reviewer for their detailed and useful comments.

References

Bar-Matthews, M., Ayalon, A., Kaufman, A., 2000. Timing and hydrological conditions of Sapropel events in the Eastern Mediterranean, as evident from speleothems, Soreq Cave, Israel. Chemical Geology 169, 145–156.

Baskaran, M., Iliffe, T.M., 1993. Age determination of recent cave deposits using excess ^{210}Pb—a new technique. Geophysical Research Letters 20, 603–606.

Berkelhammer, M., Sinha, A., Mudelsee, M., Cheng, H., Edwards, R.L., Cannariato, K., 2010. Persistent multidecadal power of the Indian summer monsoon. Earth and Planetary Science Letters 290, 166–172.

Burns, S.J., Fleitmann, D., Matter, A., Kramers, J., Al-Subbary, A.A., 2003. India Ocean climate and an absolute chronology over Dansgaard/Oeschger events 9 to 13. Science 301, 1365–1367.

Cheng, H., Edwards, R.L., Hoff, J., Gallup, C.D., Richards, D.A., Asmerom, Y., 2000. The half-lives of uranium-234 and thorium-230. Chemical Geology 169, 17–33.

Chinese Academy of Meteorological Sciences, 1981. Yearly Charts of Dryness/Wetness in China for the Last 500-Year Period, Beijing. SinoMap. Cartogr. Publ. House, Beijing (in Chinese).

Cosford, J., Qing, H., Eglington, B., Mattey, D., Yuan, D., Zhang, M., Cheng, H., 2008. East Asian monsoon variability since the Mid-Holocene recorded in a

high-resolution, absolute-dated aragonite speleothem from eastern China. Earth and Planetary Science Letters 275, 296–307.

Cosford, J., Qing, H., Mattey, D., Eglington, B., Zhang, M., 2009. Climatic and local effects on stalagmite $\delta^{13}C$ values at Lianhua Cave, China. Palaeogeography, Palaeoclimatology, Palaeoecology 280, 235–244.

Denniston, R.F., González, L.A., Asmerom, Y., Sharma, R.H., Reagan, M.K., 2000. Speleothem evidence for changes in Indian summer monsoon precipitation over the last 2300 years. Quaternary Research 53, 196–202.

Ding, Y.H., Ren, G.Y., (Eds), 2008. Scientific Introduction of Climate Change of China. Meteorological Press, Beijing, 281p. ISBN 978-7-5029-4364-6 (in Chinese).

Dykoski, C.A., Edwards, L.R., Cheng, H., Yuan, D., Cai, Y., Zhang, M., Lin, Y., Qing, J., An, Z., Revenaugh, J., 2005. A high-resolution, absolute-dated Holocene and deglacial Asian monsoon record from Dongge Cave, China. Earth and Planetary Science Letters 233, 71–86.

Fairchild, I.J., Smith, C.L., Baker, A., Fuller, L., Spötl, C., Mattey, D., McDermott, F., E.I.M.F., 2006. Modification and preservation of environmental signals in speleothems. Earth-Science Reviews 75, 105–153.

Fleitmann, D., Burns, S.J., Mudelsee, M., Neff, U., Kramers, J., Mangini, A., Matter, A., 2003. Holocene forcing of the Indian monsoon recorded in a stalagmite from southern Oman. Science 300, 1737–1739.

Fleitmann, D., Burns, S.J., Mangini, A., Mudelsee, M., Kramers, J., Villa, I., Neff, U., Al-Subbarye, A.A., Buettner, A., Hippler, D., Matter, A., 2007. Holocene ITCZ and Indian monsoon dynamics recorded in stalagmites from Oman and Yemen (Socotra). Quaternary Science Reviews 26, 170–188.

Frisia, S., Borsato, A., Fairchild, I.J., McDermott, F., Selmo, E.M., 2002. Aragonite–calcite relationships in speleothems (Grotte de Clamouse, France): environment, fabrics, and carbonate geochemistry. Journal of Sedimentary Research 72, 687–699.

Frohlich, C., Hornbach, M.J., Taylor, F.W., Shen, C.-C., Moala, A., Morton, A.E., Kruger, J., 2009. Huge erratic boulders in Tonga deposited by a prehistoric tsunami. Geology 37, 131–134.

He, X., Wang, J.L., Li, Q., Li, H.C., Li, T.Y., Cheng, H., 2007. Growth rate and the paleoclimatic significance of stalagmites in Chongqing. Carsologica Sinica 26, 196–201. in Chinese.

Henderson, G.M., 2006. Caving in to new chronologies. Science 313, 620–622.

Hu, C.Y., Henderson, G.M., Huang, J.H., Chen, Z.H., Johnson, K.R., 2008a. Report of a three-year monitoring programme at Heshang Cave, central China. International Journal of Speleology 37, 143–151.

Hu, C.Y., Henderson, G.M., Huang, J.H., Xie, S.C., Sun, Y., Johnson, K.R., 2008b. Quantification of Holocene Asian monsoon rainfall from spatially separated cave records. Earth and Planetary Science Letters 266, 221–232.

IPCC, 2007. Climate Change 2007 – The physical science basis. In: Solomon, S., Qin, D., Manning, M., Chen, Z., Marquis, M., Averyt, K.B., Tignor, M., Miller, H.L. (Eds.), Contribution of Working Group I to the Fourth Assessment Report of the Intergovernmental Panel on Climate Change. Cambridge University Press, Cambridge, United Kingdom and New York, NY, USA, 996 pp.

Ku, T.-L., Li, H.-C., 1998. Speleothems as high-resolution paleoenvironment archives: records from northeastern China. Journal of Earth System Science 107, 21–330.

Lachniet, M.S., 2009. Climatic and environmental controls on speleothem oxygen-isotope values. Quaternary Science Reviews 28, 412–432.

Lachniet, M.S., Asmerom, Y., Burns, S.J., Patterson, W.P., Polyak, V.J., Seltzer, G.O., 2004. Tropical response to the 8200 yr cold event? Speleothem isotopes indicate a weakened early Holocene monsoon in Costa Rica. Geology 32, 957–960.

Li, T.Y., 2007. The controlling factors research on the paleoenvironmental informations in stalagmite and the paleoclimate reconstruction since the last glacial period in Chongqing area. Ph.D. Dissertation. Southwest University, China (in Chinese).

Li, H.-C., Ku, T.-L., Chen, W.-J., Jiao, W.-Q., Zhao, S.-S., Chen, T.-M., Li, T.-Y., 1996. Isotope studies of Shihua Cave, Beijing – II: radiocarbon dating and age correction of stalagmite. Seismology and Geology 18, 329–338.

Li, H.-C., Ku, T.-L., Stott, L.D., Chen, W.J., 1998. Applications of interannual-resolution stable isotope records of speleothem: climatic changes in Beijing and Tianjin, China during the past 500 years – the $\delta^{18}O$ record. Science in China 41, 362–368.

Li, H.-C., Ku, T.-L., You, C.F., Cheng, H., Edwards, R.L., Ma, Z.B., Tsai, W.S., Li, M.D., 2005. $^{87}Sr/^{86}Sr$ and Sr/Ca in speleothems for paleoclimate reconstruction in central China between 70 and 280 k yr ago. Geochimica et Cosmochimica Acta 69, 3933–3947.

Li, T.Y., Li, H.-C., Yuan, D.X., Wang, J.L., Yang, Y., Wang, X.Y., Li, Y.J., Qin, J.M., Zhang, M.L., Lin, Y.S., 2006. Climatic variability in Chongqing, China during the past 4500 years reflected by a stalagmite record from Xinya Cave. Carsologica Sinica 25, 95–100 (in Chinese).

Li, T.Y., Yuan, D.X., Li, H.-C., Yang, Y., Wang, J.L., Wang, X.Y., Li, J.Y., Qin, J.M., Zhang, M.L., Lin, Y.S., 2007. High-resolution climate variability of southwest China during 57–70 ka reflected in a stalagmite $\delta^{18}O$ record from Xinya cave. Science in China Series D: Earth Sciences 50, 1202–1208.

Li, Q., Wang, J.L., Li, H.-C., Ye, M.Y., Wang, Y., Li, T.Y., He, X., 2008a. Climatic significance of the Mg/Ca ratio from speleothems in Chongqing. Carsologica Sinica 27, 145–150 (in Chinese).

Li, T.Y., Li, H.-C., Li, Y.J., Yuan, D.X., Wang, J.L., Ye, M.Y., Tang, L.L., Shen, C.C., WC, A.S.H.I., 2008b. The $\delta^{13}C$ and $\delta^{18}O$ features and their significances of speleothems in Furong Cave, Chongqing, China. Geological Review 54, 712–720 (in Chinese).

Liu, Y.H., Hu, C.Y., Huang, J.H., Xie, S.C., Chen, Z.H., 2005. The research of the layer thickness of the stalagmite from the middle reaches of the Yangtze River taken as an proxy of the east Asian summer monsoon intensity. Quaternary Sciences 25, 228–234 (in Chinese).

McDermott, F., 2004. Palaeo-climate reconstruction from stable isotope variations in speleothems: a review. Quaternary Science Reviews 23, 901–918.

Patterson, W.P., Smith, G.R., Lohmann, K.C., 1993. Continental paleothermometry and seasonality using the isotopic composition of aragonite otoliths of freshwater fishes. In: Swart, P.K., Lohmann, C.K., Mckenzie, J., SavinClimate, S. Change in Continental Isotopic Records (Eds.). Geophysical Monograph Series, vol. 78, pp. 191–202.

Paulsen, D.E., Li, H.-C., Ku, T.-L., 2003. Climate variability in central China over the last 1270 years revealed by high-resolution stalagmite records. Quaternary Science Reviews 22, 691–701.

Polyak, V.J., Asmerom, Y., 2001. Late Holocene climate and cultural changes in the Southwestern United States. Science 294, 148–151.

Shen, C.C., Edwards, R.L., Cheng, H., Dorale, J.A., Thomas, R.B., Moran, S.B., Weinstein, S.E., 2002. Uranium and thorium isotopic and concentration measurements by magnetic sector inductively coupled plasma mass spectrometry. Chemical Geology 185, 165–178.

Shen, C.-C., Cheng, H., Edwards, R.L., Moran, S.B., Edmonds, H.N., Hoff, J.A., Thomas, R.B., 2003. Measurement of attogram quantities of ^{231}Pa in dissolved and particulate fractions of seawater by isotope dilution thermal ionization mass spectroscopy. Analytical Chemistry 75, 1075–1079.

Shen, C.-C., Li, K.-S., Sieh, K., Natawidjaja, D., Cheng, H., Wang, X., Edwards, R.L., Lam, D.D., Hsieh, Y.-T., Fan, T.-Y., Meltzner, A.J., Taylor, F.W., Quinn, T.M., Chiang, H.-W., Kilbourne, K.H., 2008. Variation of initial $^{230}Th/^{232}Th$ and limits of high precision U–Th dating of shallow-water corals. Geochimica et Cosmochimica Acta 72, 4201–4223.

Tan, M., Hou, J.Z., Cheng, H., 2002. Methodology of quantitatively reconstructing paleoclimate from annually laminated stalagmites. Quaternary Sciences 22, 209–219 (in Chinese).

Wang, B., 2006. The Asian Monsoon. Springer-Praxis Publishing Ltd., Chichester, UK. 787p.

Wang, Y.J., Cheng, H., Edwards, R.L., An, Z.S., Wu, J.Y., Shen, C.-C., Dorale, J.A., 2001. A high-resolution absolute-dated late Pleistocene monsoon record from Hulu Cave, China. Science 294, 2345–2348.

Wang, Y.J., Cheng, H., Edwards, R.L., He, Y., Kong, X., An, Z., Wu, J., Kelly, M.J., Dykoski, C.A., Li, X., 2005. The Holocene Asian monsoon: links to solar changes and north Atlantic climate. Science 308, 854–857.

Wang, Y.J., Cheng, H., Edwards, R.L., Kong, X., Shao, X., Chen, S., Wu, J., Jiang, X., Wang, X., An, Z., 2008. Millennial- and orbital-scale changes in the east Asian monsoon over the past 224,000 years. Nature 451, 1090–1093.

Yuan, D.X., Cheng, H., Edwards, R.L., Dykoski, C.A., Kelly, M.J., Zhang, M.L., Qing, J.M., Lin, Y.S., Wang, Y.J., Wu, J.Y., Dorale, J.A., An, Z.S., Cai, Y.J., 2004. Timing, duration, and transition of the last interglacial Asian monsoon. Science 304, 575–578.

Zhang, D.E., Li, X.Q., Liang, Y.Y., 2003. Continuation (1992–2000) of the yearly charts of dryness/wetness in China for the last 500 years period. Journal of Applied Meteorological Science 14, 379–388 (in Chinese).

Zhang, P.Z., Cheng, H., Edwards, R.L., Chen, F.H., Wang, Y.J., Yang, X.L., Liu, J.A., Tan, M., Wang, X.F., Liu, J.H., An, C.L., Dai, Z.B., Zhou, J., Zhang, D.Z., Jia, J.H., Jin, L.Y., Johnson, K.R., 2008. A test of climate, sun, and culture relationships from an 1810-year Chinese cave record. Science 322, 940–942.

Zhang, D.E., Li, H.-C., Ku, T.-L., Lu, L.H., 2010. On linking climate to Chinese dynastic change: Spatial and temporal variations of monsoonal rain. Chinese Science Bulletin 55, 77–83.